Degradation of RSP/PM Al-8Fe-4Ce during Creep

R.K. Mahidhara

The creep behavior of Al-8Fe-4Ce powder metallurgy alloy produced by rapid solidification processing (RSP/PM alloy) was studied within the 623 to 773 K temperature range and at initial stresses ranging from 10 to 52 MPa. The activation energy, Q, for creep in RSP/PM Al-Fe-Ce alloy is $2.3Q_L$, where Q_L is the activation energy for lattice diffusion in pure aluminum and the stress exponent is 8.6. The high-temperature creep deformation is associated with deformation of matrix and $Al_{13}Fe_4$ incoherent particles. In addition, particle coarsening is an important factor in alloy degradation. The formation and growth of cavities during creep at all stress levels at 698 K is also a contributing factor.

Keywords
aluminum alloys, creep testing, powder metallurgy, rapid solidification processing

1. Introduction

DISPERSION-HARDENED creep-resistant alloys are an important class of elevated-temperature materials. The creep resistance of dispersion-hardened alloys is affected both by matrix strength and by the size, morphology, and volume fraction of the dispersed phase particles. The stability of the matrix and of the second phase also influences creep resistance.

Rapid solidification processing (RSP) is a viable method of producing dispersion-strengthened alloys. Much work has focused on aluminum and titanium alloys for elevated-temperature applications. Among the aluminum-base RSP alloys for elevated-temperature use, Al-Fe-Ce is considered an important candidate (Ref 1). This alloy exhibits good thermal stability and strength at temperatures lower than 723 K. Above 723 K, however, the strength falls dramatically with increasing temperature due to coarsening and deformation of particles (Ref 2, 3). The high-temperature deformation mechanisms in this alloy within the temperature range of 523 to 623 K and in the stress range of 20 to 115 MPa have been reported (Ref 4, 5). The objective of this paper is to study systematically the creep behavior of Al-Fe-Ce powder metallurgy alloy (RSP/PM alloy) at a test temperature of 698 K, which corresponds to 0.7 T_M, where T_M is the liquidus temperature of the alloy.

2. Experimental Procedure

Al-8.7Fe-4Ce was obtained from ALCOA. Gas-atomized powders of that composition were consolidated by cold compaction followed by vacuum hot pressing and extrusion. Flat tensile specimens with a gage length of 25.4 mm were machined from the as-received material and polished. These specimens had their tensile axes parallel to the extrusion direction.

Two types of creep tests were performed under dead load conditions. In one type, tests were carried out at 623, 698, and 773 K in the stress range of 10 to 52 MPa. The stress acting on the specimen was incrementally changed from an initial level of 10 MPa up to the maximum permissible stress of 52 MPa. This was followed by decremental changes in stress from 52 to 10 MPa on the same specimen. Before any change in stress level was made, it was ensured that steady-state creep behavior was definitely achieved at the previous stress level.

In the second type of creep test, some of the specimens were crept at one particular stress to a possible failure at 698 K. The level of cavitation and changes in particle size of crept specimens were determined using carbon extraction replicas taken from the polished specimens. Johnson-Saltykov size distributions were performed on cavities by assuming that the cavities were spherical in shape (Ref 6). Density measurements with ±96% accuracy were performed on crept specimens to assess the level of cavitation. Metallography involved transmission and scanning electron microscopy (TEM and SEM) on both the undeformed and deformed specimens. Samples for TEM were electrolytically thinned in a solution of 20% nitric acid and 80% methanol at 243 K. These samples were then examined in a 700H Hitachi TEM operating at 200 keV. Fractography was performed using SEM.

3. Results and Discussion

3.1 *Creep Behavior*

Figure 1 is a transmission electron micrograph of the as-received alloy. The microstructure essentially contained heavily faulted incoherent particles (0.17 to 0.22 μm in size) and subgrains (0.5 to 0.8 μm in size). The volume fraction of the $Al_{13}Fe_4$ and $Al_{10}Fe_2Ce$ particles together was about 0.23.

Figure 2 is a log-lot plot of strain rate ($\dot{\varepsilon}$) normalized by temperature-compensated lattice diffusion coefficient (D_L) versus flow stress (σ) normalized by temperature-compensated elastic modulus (G). Both the temperature-compensated lattice diffusion coefficient and elastic modulus corresponded to those for pure aluminum. The plot in Fig. 2 also includes compression creep data of Yaney et al. (Ref 2, 3) at 598, 623, and 723 K as well as tensile creep data of Legzdina and Parthasarathy (Ref 4) at their maximum test temperature of 623 K. From the slope of log $\dot{\varepsilon}/D$ versus log σ/G, the temperature-dependent stress exponent, n, was evaluated. It has a value of 8.6 within the 623 to 773 K temperature range. In rapidly solidified Al-Fe-Ce (Ref 4) and Al-Zr-V (Ref 7) alloys, higher values of stress exponents within the power-law creep regime were reduced to 4.4 (the stress exponent for pure aluminum) by introducing a threshold stress. Following the stress change tests, the particle and grain size were measured. At 698 K, particle size and grain size in-

R.K. Mahidhara, Tessera Inc., San Jose, CA 95134, USA.

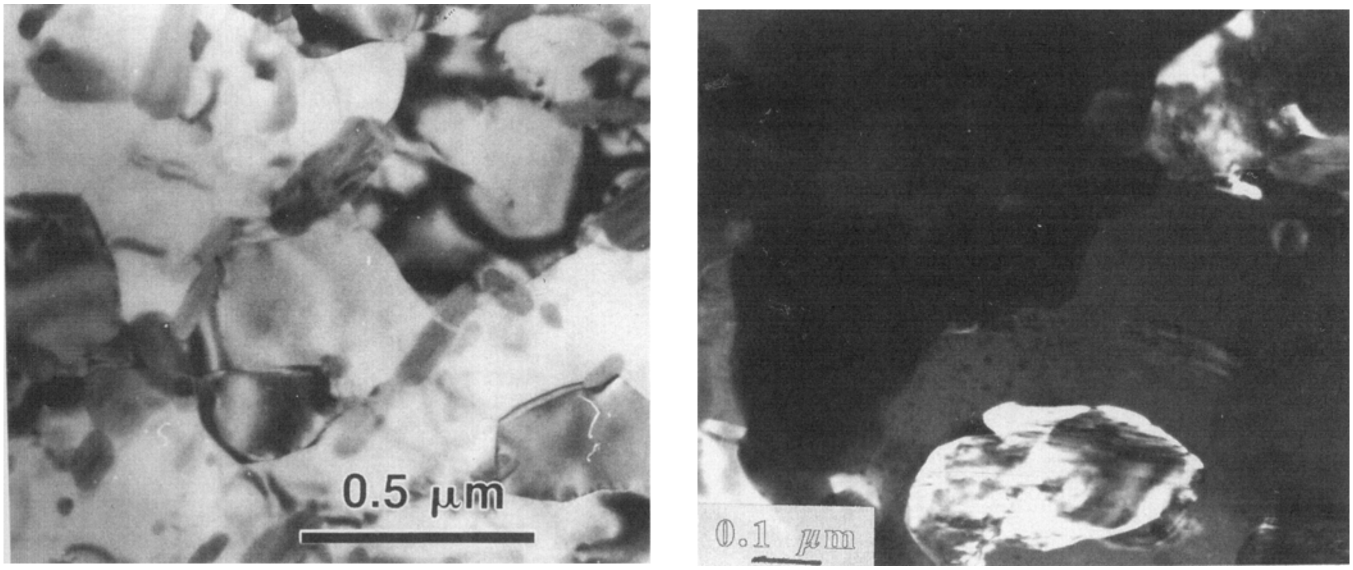

(a) (b)

Fig. 1 Transmission electron micrographs of the as-received RSP/PM Al-Fe-Ce alloy in bright field (a) and dark field (b) of monoclinic $Al_{13}Fe_4$ intermetallic using (001) reflection

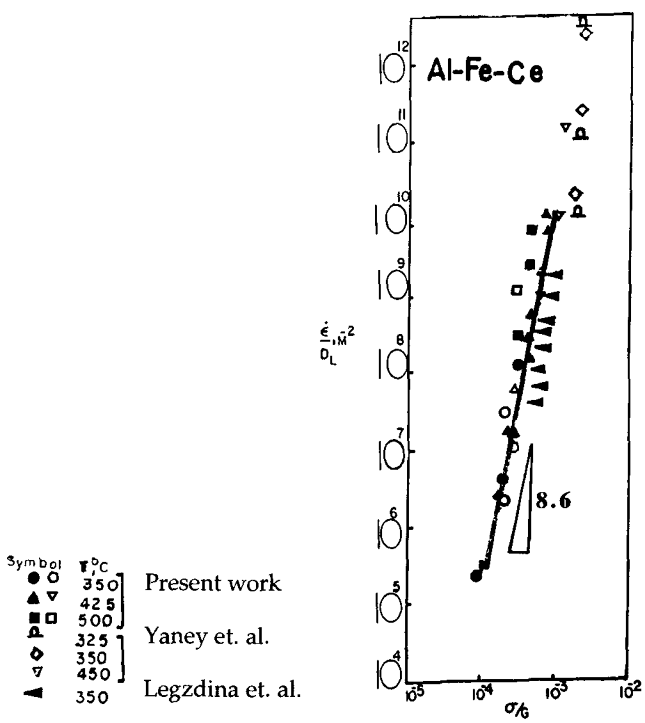

Fig. 2 Plot of normalized stress versus normalized strain rate for the RSP/PM Al-Fe-Ce alloy. The open symbols correspond to a test conducted during decremental loading, and the closed symbols correspond to a test conducted during incremental loading.

creased by only a factor of 1.20 and 1.10, respectively, over a 50 to 60 h testing period, thereby ensuring stable microstructure.

The activation energy for the creep deformation was obtained by using the well-known Dorn equation (Ref 8). From a plot of log ($\dot{\varepsilon}G^{n-1}T$) versus $1/T$ shown in Fig. 3, the activation energy for the creep deformation in the temperature range of 623 to 773 K was found to be 309.2 kJ/mole, which is 2.3 times that for lattice diffusion (Q_L) in aluminum solid solution. Yaney et al. (Ref 2, 3) have identified two different regimes that depend on testing temperature, on the basis of compression creep tests on RSP/PM Al-Fe-Ce alloy. Within the 523 to 573 K temperature range, the average value of n is 22 and activation energy for creep is 1.4 times the activation energy for self-diffusion for pure aluminum (Q_{SD}), which is 142 kJ/mole. However, when the test temperature is in the range of 723 to 773 K, n corresponds to 8.2 and the activation energy for creep is 3.4 Q_{SD}. Based on their creep data, Yaney et al. (Ref 2, 3) considered a temperature of 723 K, below which RSP/PM Al-Fe-Ce is stronger than oxide-dispersion-strengthened alloy and vice versa. The loss of strength at temperatures greater than 723 K has been attributed to the simultaneous deformation of $Al_{13}Fe_4$ particles and the matrix, in addition to microstructural instability due to particle coarsening with possible changes in their volume fraction (particularly at the highest test temperature of 773 K). In contrast, Angers et al. (Ref 5) have found no volume changes of the particulates in specimens crept at 698 K, although considerable particle coarsening was reported at this temperature due to enhancement in excess vacancies and dislocation activity. Since the stress exponent is 8.6 and activation energy for high-temperature flow is $2.3Q_L$, the mechanism of high-temperature flow in the present study also is associated with deformation of matrix and incoherent particles.

In addition to incremental tests, uniaxial creep tests were conducted at 698 K and at an initial stress of 10 MPa. The steady-state creep rate was 5×10^{-9}/s, and the grain size and particle size increased by a factor of 3.5 and 6, respectively, after 100 h of testing. At an initial stress of 17.25 MPa, the steady-

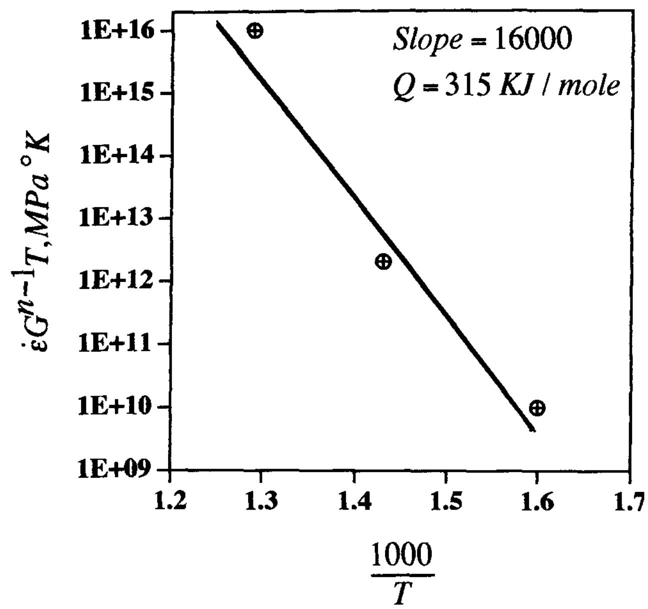

Fig. 3 Activation energy plot for the RSP/PM Al-Fe-Ce alloy

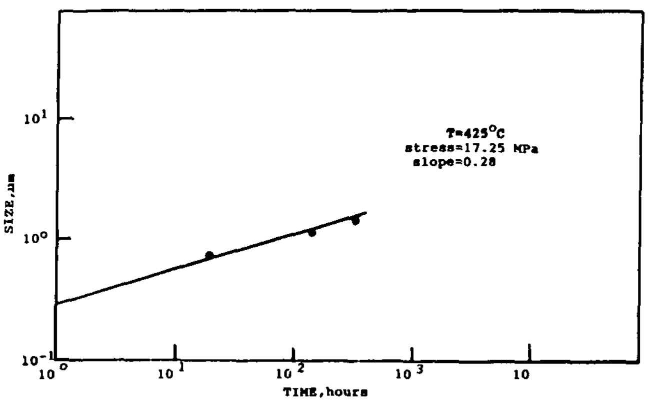

Fig. 4 Plot of subgrain size versus deformation time at an initial stress of 17.25 MPa and a temperature of 698 K

state creep rate was 1×10^{-8}/s, and the grain size and particle size changed by an approximate factor of 2 after 100 h of testing.

The variation in grain size during creep is shown in Fig. 4 for a specimen tested at an initial stress of 17.25 MPa and a temperature of 698 K for 360 h. This graph suggests that, in addition to particle coarsening due to creep at 698 K akin to that reported by Angers et al. (Ref 5), microstructural changes due to grain coarsening may also contribute to alloy softening during 698 K creep. The grain growth may be due to the loss of associated Zener drag effect of the particles over the boundaries. Generally, an increase in grain size is helpful as it increases alloy creep resistance. However, a concomitant increase in average particle size will result in an increase in the interparticle spacing, with a corresponding decrease in Orowan stress for dislocations to bypass the particles. This can offset the virtues of grain coarsening to cause alloy softening during high-temperature flow. The transmission electron micrograph of the deformed sample in Fig. 5 suggests that dislocation activity

Fig. 5 Transmission electron micrograph of RSP/PM Al-Fe-Ce alloy deformed at an initial stress of 17.25 MPa and a temperature of 698 K for 360 h

occurs during high-temperature flow. This is not uncommon in particle-strengthened aluminum-base alloys such as Al-Fe-Ce.

Therefore, the present data, collected at a slightly lower temperature of 698 K, would suggest that the alloy possibly may be weaker due to simultaneous particulate and matrix deformation as evidenced by a stress exponent of 8.6 and higher activation energy for creep together with microstructural changes brought about by particle coarsening (which supersedes the effect of grain coarsening). Particulate deformation and coarsening are probably the dominant contributors to alloy softening. Another important factor to consider is cavitation.

3.2 *Failure Process*

At 698 K, cavitation was evident in specimens that were tested at an initial stress of less than 27.75 MPa after 360 h. In addition, a specimen crept at a stress of 27.75 MPa (steady-state creep rate was 1×10^{-8}/s) failed with a 10% reduction in area. The density of the crept specimen changed by as much as 0.6% at this stress. This conclusion was reached following density measurements on a specific length of the gage section taken from the broken area. Results were compared with those for a virgin specimen, and a fractographic examination was conducted.

Lack of relaxation of stress concentrations by diffusion processes at grain-boundary particles on sliding boundaries will lead to creep damage by nucleation and growth of cavities (Ref 9). The cavities grow on further deformation by either power-law creep (Ref 10) or by coupled grain-boundary diffusion and dislocation creep (Ref 9), the rate of which is enhanced by grain-boundary sliding (Ref 11). Cavity coalescence is dependent on the damage parameter, which is the ratio of

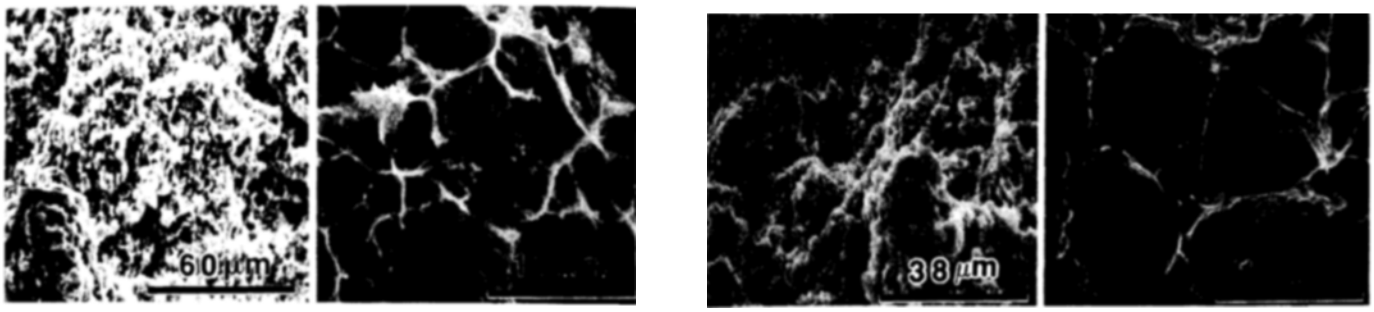

(a) (b)

Fig. 6 Fracture surfaces of specimens crept at a temperature of 698 K and an initial stress of 27.75 MPa (a) and 52.18 MPa (b) at lower (left) and higher (right) magnifications

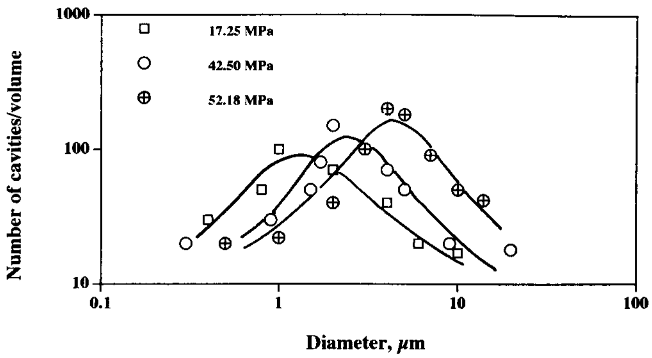

Fig. 7 Distribution of cavities in RSP/PM Al-8.7Fe-4Ce

cavity size and cavity spacing (Ref 12), and leads to ultimate failure. The lumpy fracture surface shown in Fig. 6(a) was taken from a sample tested at an initial stress of 27.75 MPa and suggests that Al-Fe-Ce failed by an intergranular mechanism. In addition, grain size decreased by a factor of 1.2 due to recrystallization with no significant change in particle size. Thus, another source of weakening at 698 K in Al-Fe-Ce during deformation could be cavitation. Cavity size distribution at 17.25 MPa is shown in Fig. 7.

At initial stress levels of 42.5 MPa (which corresponds to a steady-state creep rate of 1×10^{-5}/s and a reduction in area of 20%) and 52.18 MPa (which corresponds to a steady-state creep rate of 1×10^{-4}/s and a reduction in area of 40%), profuse cavitation (1.0 and 1.25%, respectively) and a decrease in grain size were observed. Figure 6(b) corresponds to the fracture surface of the specimen crept at an initial stress of 52.18 MPa. The fracture surface appears lumpy and contains both small and shallow cavities that formed by decohesion of hard intermetallic particles at the particle-matrix interface with no evidence of particle coarsening. The stress concentration in these regions caused the failure to occur by rapid crack propagation as a consequence of power-law creep, resulting in microdimples (Fig. 6b).

Furthermore, as Fig. 7 shows, at an initial stress of 52.18 MPa the average cavity size and number of cavities per unit volume of the alloy are higher than at 42.5 or 17.25 MPa. This is related to the higher rates of nucleation, growth, and coalescence of cavities at higher stress levels due to the operating power-law creep mechanism. Therefore, in addition to particle and matrix deformation and coarsening of hard particles, the formation and growth of cavities by decohesion during high-temperature flow is also responsible for the degradation of RSP/PM Al-Fe-Ce alloy.

4. Conclusions

- Since the activation energy, Q, for creep in RSP/PM Al-Fe-Ce alloy is $2.3Q_L$ and the stress exponent is 8.6, high-temperature creep is associated with matrix and particle deformation, which are responsible for alloy degradation at 698 K during creep.
- At 698 K, microstructural changes occurred during creep deformation at initial stresses up to 17.25 MPa. Particle coarsening is an important contributor to alloy degradation.
- At 698 K, cavities were observed in crept specimens at all stress levels. Thus, cavitation is also an important factor in the degradation of RSP/PM Al-Fe-Ce alloy.

References

1. J. Ekvall, R. Rainen, D. Chellman, and R. Flores, *J. Aircraft*, Vol 27, 1990, p 836-843
2. D.L. Yaney and W.D. Nix, *Metall. Trans.*, Vol 18A, 1987, p 893-902
3. D.L. Yaney, J.C. Gibeling, and W.D. Nix, *Proc. 7th Int. Conf. Strength of Metals and Alloys (ICSMA7)*, D.M.R. Taplin, P. Rama Rao, J.F. Knott, and R. Valluri, Ed., Pergamon Press, Oxford, 1985, p 887-892
4. D. Legzdina and T.A. Parthasarathy, *Metall. Trans.*, Vol 18A, 1987, p 1713-1719
5. L. Angers, M.E. Fine, and J.R. Weertman, *Metall. Trans.*, Vol 18A, 1987, p 555-561
6. E.E. Underwood, in *Quantitative Microscopy*, R.T. DeHoff and F.N. Rhines, Ed., McGraw Hill Publishers, New York, NY, 1968, p 169
7. Y.C. Chen, M.E. Fine, and J.R. Weertman, *Acta Metall. Mater.*, Vol 5, 1990, p 713-724
8. J.E. Bird, A.K. Mukherjee, and J.E.Dorn, *Trans. ASM*, Vol 62, 1969, p 155-175
9. V. Tvergaard, *Acta Metall.*, Vol 32, 1984, p 1977-1989
10. R. Raj, *Acta Metall.*, Vol 26, 1978, p 341-352
11. K.J. Hsia, D.M. Parks, and A.S. Argon, *Mech. Mater.*, Vol 11, 1991, p 43-60
12. V. Tvergaard, *Adv. Appl. Mech.*, Vol 27, 1985, p 83-102